Quantum Control of the Photodissociation of Sodium Iodide

Kunihito Hoki, Yukiyoshi Ohtsuki, Hirohiko Kono, Yuichi Fujimura,* and Shiro Koseki†

Department of Chemistry, Graduate School of Science, Tohoku University, Sendai 980-8578

†Chemistry Department for Materials, Faculty of Engineering, Mie University, 1515 Kamihama, Tsu 514-0008

(Received July 7, 1999)

A quantum control of photodissocation of NaI to neutral atom fragments, NaI → NaI* → Na+I, was theoretically studied by using a locally optimized control method. The purpose of this control was to obtain as many neutral fragments as possible within one cycle of the nuclear vibration. The control was based on a pump-and-dump scheme. Weak and strong laser-field cases were used. The optimal dump pulses in both cases were shown to be of a linear time-dependent up-chirp type by analyzing their time- and frequency-resolved power spectra. This confirms the result predicted using a non-optimal control method in a previous paper (*Chem. Phys. Lett.*, **231**, 50 (1994)). The nuclear wavepacket propagations were also analyzed to see how photodissociation takes place when controlled pulses are used.

Quantum control is a new research field of chemical reaction dynamics[1—5] which utilizes the coherent interaction between laser fields and vibrational wavepackets of the molecule under consideration. It is possible to obtain higher yields of a reaction product using quantum control than using incoherent control methods, such as ordinal photochemical reactions. This is because wavepackets can be transferred more effectively by tailored laser pulses in quantum control.[6—13] Tailored laser pulses are designed on the basis of an optimal control theory.[14—35]

The purpose of this study was to apply a locally optimized control method developed by us to the photodissociation of NaI. This system is a typical example of nonadiabatic transitions induced by an optical transition.[36—42] There have been several studies on the quantum control of this system.[42—47] In a previous study,[48] we designed pulses to increase the nonadiabatic transition rate between the two adiabatic states by controlling the velocity of nuclear wave packets on the upper adiabatic potential. In this study, we hoped to clarify what kinds of pulses are needed to produce neutral products within one cycle of nuclear motion. That is, we wanted to control the photodissociation yields of NaI induced by laser pulses, rather than the nonadiabatic transition, itself. For this purpose, we used a pump-dump control scheme. The affects of the nonadiabatic transition were taken into account in solving the optimized pulses of the photodissociation.

In a previous paper,[44] we predicted laser pulses that would produce an efficient photodissociation product, NaI* → Na+I, within hundred-femtosecond time regime, corresponding to a half cycle of the nuclear vibration. In that calculation, a non-optimal control method was used. It was shown that up-chirp pulses can produce a highly efficient yield of the photodissociation product. In this paper, we report on the control pulses that were designed using a locally optimized control method.[34] Furthermore we verify that the resulting dump pulse is a linear time-dependent up-chirp pulse. The characteristic features of the pulse are also discussed.

In the next section, we briefly describe wavepacket treatment of NaI photodissociation and our optimization method for pump-and-dump control of the photodissociation. Then, we present the results of quantum control of NaI photodissociation using weak and strong laser fields. Finally, we discuss the different behaviors in the photodissociation control between the two cases in terms of nuclear wave packet propagation dynamics.

Theoretical

NaI Dynamics. Consider quantum control of NaI photodissociation by a pump-and-dump scheme within a two-electronic-state model, as shown in Fig. 1. The adiabatic potential curves associated with the photodissociation are shown in Fig. 1. The time development of NaI in the electronic field ($E(t)$) within the dipole approximation is determined by solving the time-dependent Schrödinger equation,

$$i\hbar\frac{\partial}{\partial t}|\psi(t)\rangle = [H_M - \mu E(t)]|\psi(t)\rangle, \quad (1)$$

where H_M is the molecular Hamiltonian

$$H_M = T_N + H_{el} \quad (2)$$

in which T_N and H_{el} denote the nuclear kinetic energy operator and the electronic Hamiltonian, respectively; μ is the electric dipole moment. Let the adiabatic electronic states be denoted as $|S_0(R)\rangle$ and $|S_1(R)\rangle$, where R denotes the parametric dependence of the electronic states on the nuclear coordinate R. It is convenient to adopt the diabatic basis set ($|i(R)\rangle$ and $|c(R)\rangle$ to solve Eq. 1. $|i(R)\rangle$ and $|c(R)\rangle$ are called the ionic state and covalent state, respectively, in the valence-bond representation. By expanding the time-dependent Schrödinger Eq. 1 in terms of the diabatic basis set, we obtain the following coupled equations for nuclear wave packets, $X_i(R,t)$ and $X_c(R,t)$:

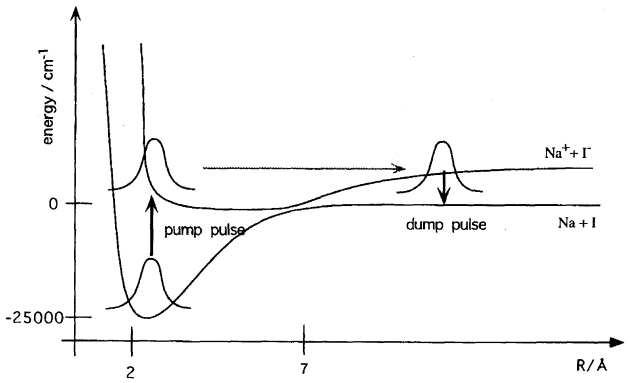

Fig. 1. A pump-dump pulse control of photodissociation yields within one cycle of the nuclear motion. The potential energy curves of the ground state($X^1\sum$) and excited electronic state ($B^1\sum^+$) associated with the photodissociation are shown in the adiabatic representation. Their two potential curves interact with each other due to nonadiabatic coupling.

$$i\hbar\frac{\partial}{\partial t}X_i(R,t)=\left[-\frac{\hbar^2}{2M}\frac{\partial^2}{\partial R^2}+V_{ii}(R)\right]X_i(R,t) +(V_{ic}(R)-\mu_{ic}(R)E(t))X_c(R,t), \quad (3a)$$

and

$$i\hbar\frac{\partial}{\partial t}X_c(R,t)=\left[-\frac{\hbar^2}{2M}\frac{\partial^2}{\partial R^2}+V_{cc}(R)\right]X_c(R,t) +(V_{ci}(R)-\mu_{ci}(R)E(t))X_i(R,t), \quad (3b)$$

where M is the reduced mass of NaI, and $X_i(R,t)=\langle iR|\psi(t)\rangle$ and $X_c(R,t)=\langle cR|\psi(t)\rangle$ are the nuclear wavepackets on the ionic and covalent potential surfaces, respectively. Here, $|iR\rangle=|i(R)\rangle|R\rangle$ and $|cR\rangle=|c(R)\rangle|R\rangle$ in which $|R\rangle$ is the eigenvector of nuclear coordinate R. In Eqs. 3 and 3b, $V_{ii}(R)$ is the potential energy of the ionic electronic state and $V_{cc}(R)$ is that of the covalent state. $V_{ci}(R)(V_{ic}(R))$ is the coupling matrix element between the ionic and covalent electronic states, and is defined as

$$V_{ci}(R)=\int dR'\langle cR|H_{el}|iR'\rangle=\langle c(R)|H_{el}(R)|i(R)\rangle, \quad (4)$$

where $H_{el}(R)$ denotes the electronic Hamiltonian of NaI in the nuclei coordinate representation.

In Eq. 3, $\mu_{ci}(R)(\mu_{ic}(R))$ is the electric dipole moment. These coupling matrix elements were evaluated using ab initio molecular orbital program codes, GAMESS[49] and MOLPRO.[50] In our dynamics calculation, the R-dependence of the electric dipole moments between the ground state ($X^1\sum^+$) and the second excited state ($B^1\sum^+$) was modified in a way that the peak position (5.743 Å) of the dipole moments was moved to the crossing point (R_c), estimated by experiments, and that the shape of the dipole moment function was maintained. The peak position of the nonadiabatic coupling matrix element between these electronic states is also shifted to the crossing point R_c. These modifications may be explained by the existence of strong spin-orbit couplings among the low-lying electronic states: When the spin-orbit coupling is considered in the molecular orbital calculations, the avoided crossing occurs among the potential energy curves of the low-lying spin-mixed states in the region of $R=5.5$ Å and 7 Å. Although these coupling matrix elements should be transformed into the spin-mixed space, the above modification has been introduced for simplicity, instead of an exact transformation into the spin-mixed space.

The wave packet $X_{S_0}(R,t)$ on the adiabatic potential in the electronic ground state and $X_{S_1}(R,t)$ on the excited state are easily obtained from the diabatic basis set $X_i(R,t)$ and $X_c(R,t)$ as

$$X_a(R,t)=\sum_d \Lambda^*_{da}(R)X_d(R,t), \quad (5)$$

where $d=c$ and i, and $a=S_0$ and S_1, respectively. $\Lambda^*_{da}(R)$ is the transformation coefficient, and is defined as $\Lambda^*_{da}(R)=\langle a(R)|d(R)\rangle$.

Locally Optimized Laser Field. Consider a target operator W whose expectation value we want to maximize at time t_f by a laser field $E(t)$. The optimal laser field is given in the general optimized control theory as

$$E(t)=-2A\mathrm{Im}\langle\psi(t_f)|WU(t_f,t)\mu|\psi(t_f)\rangle, \quad (6)$$

where A is a positive constant, and $U(t_f,t)$ is a unitary operator. The unitary operator is defined as

$$U(t_f,t)=\hat{T}\exp\left[-\frac{i}{\hbar}\int^{t_f}dt\{H_M-\mu E(t)\}\right], \quad (7)$$

where $\hat{T}$ is the time-ordering operator. Equation 6 is a global optimization expression, and shows that the optimized field at time t depends on time t_f. In order to avoid complexities involved with global optimization, we used a local optimization procedure. We divided the time development from the initial to the final time into short time steps, and carried out optimization at each short time step.[25,34] If the target operator is satisfied by the relation

$$\langle\psi(t)|[H_M,W]|\psi(t)\rangle=0, \quad (8)$$

where [,] is a commutator, the optimized field at each step is expressed as[34]

$$E(t)=-2A\mathrm{Im}\langle\psi(t)|W\mu|\psi(t)\rangle. \quad (9)$$

This is an expression for the locally designed optimal laser field.

Results and Discussion

In order to obtain as much neutral product of photodissociation of NaI as possible within one cycle of the nuclear vibration, we chose the following form as the target operator (W) in the pump and dump scheme:

$$W=|i_0\rangle W_p\langle i_0|+\int dR|cR\rangle W_d\langle cR|, \quad (10)$$

where $|i_0\rangle$ is the lowest vibrational state in the ground ionic electronic state. In Eq. 10, the first term is associated with the pumping process, and the second one with the dumping process. W_p was taken to have a negative value to ensure the generation of a pumping pulse. W_d was taken to have a

positive value and the integration range was taken from the outside of the internuclear distance of $R = 9.5$ Å to infinity, but for practical reasons, we set an absorbing boundary.

Two cases were considered according to the intensities of the pump-and-dump pulses used: that is, maximum field strengths of ca. 10^9 V m^{-1} and ca. 10^8 V m^{-1}. In the former case, the population was almost completely transferred from the initial state to the excited state. On the other hand, in the latter case, the population transfer was low, and the population in the ground state was larger than that in the excited state. We designated these strong and weak field cases, respectively.

Strong Field Case. Figure 2 shows locally designed optimal pulses applied to NaI photodissociation in the strong-field case. The maximum field strength of 6×10^9 V m^{-1} corresponds to a peak intensity of 4.8 TW cm^{-2}. The inserted figure is the time- and frequency-resolved power spectrum of the dump pulse. The dump pulse consists of only a few cycle pulses, which slightly increases the difficulty of the analysis, but the pulse can be approximately expressed by a form whose central frequency is a linearly increasing function of time, that is, an up-chirp pulse, as indicated by a straight line as a guide. Such a linear up-chirp laser pulse makes the wavepacket moving along the excited-state potential effectively transfer to the ground state potential. As shown in Fig. 1, the energy difference between these two potentials beyond their crossing point increases approximately linearly as the distance increases. Applications of chirped pulses to the quantum control of molecular dynamics have been proposed by several researchers.[51,53]

Figure 3 shows the time evolution of the populations in the locally designed optimal pulses in the strong field case. The unbroken line denotes the population in the electronically excited state, and the broken line the photodissociation product from the excited state induced by the controlled pulse. We can see that almost all of the population in the initial

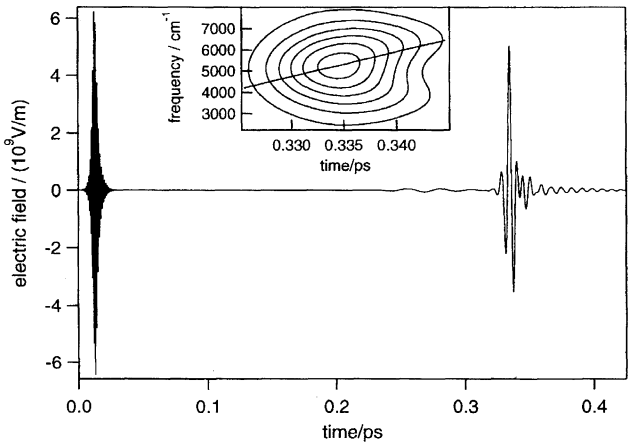

Fig. 2. Locally designed optimal pulses in a strong field case. The maximum field strength is set to be 6×10^9 V m^{-1}. The inserted figure shows the time- and frequency-resolved spectrum of the dump pulse. The optimal pulse is a linear time-dependent, up-chirp pulse as indicated by a straight line as a guide.

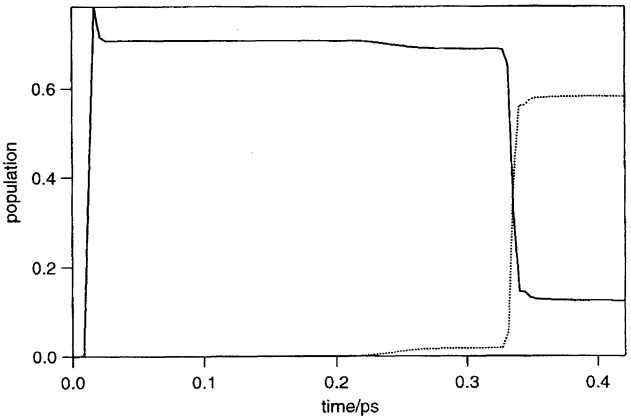

Fig. 3. The time evolution of the populations in the strong field case. The undotted line denotes the population in the electronically excited state, and the dotted line the photodissociation product from the excited state induced by the optimal dump pulse.

state was transferred into the excited state by the optimized pump pulse, and that about 60% yields of photodissociation is produced by the controlled dump pulse within one cycle of NaI-stretching vibrational motion. A small increase in the population starting after 200 fs is due to the spontaneous predissociation induced by the nonadiabatic coupling between the two adiabatic states. A spire at the initial time stage in Fig. 3 originated from a stimulated emission during the pumping process because a strong input laser field was applied. A strong pulse has been reported to localize the wavepacket.[54]

Figure 4 shows the time evolution of the population in the S_0-ionized state in the diabatic representation. We can see coherent motion and quantum beats at $R \approx 2$ Å in the ground-ionized state. These behaviors are due to the stimulated emission used to produce vibrational coherence in the ground state. Such a stimulated emission process can be utilized to obtain a higher velocity in the excited electronic state, which in turn can induce a higher probability of nonadiabatic transition. This is the principle used to control the nonadiabatic transition of NaI.[48] The disappearance of the wavepacket of the ionic component at $R \approx 10$ Å in Fig. 4 originates from the transition to the dissociative covalent state, which is induced by the optimized linear up-chirp pulse.

Figure 5a shows the time evolution of the nuclear wavepacket of NaI on the ground state and Fig. 5b that on the S_1 state in the strong field case. The ordinate denotes the absolute value of the nuclear wavepackets. The time-evolution of the wavepackets in Fig. 5 demonstrates the manner in which the wavepackets are transferred by the controlled pump and dump pulses, and shows that the dump pulse effectively transfers the wavepacket in the excited state to that in the ground state.

We would like to comment on the possibility of tunneling ionization induced by potential distortion in the presence of laser pulses of ca. 10^9 V m^{-1}. It is well known that tunneling ionization makes a significant contribution when $\gamma < 1$ in

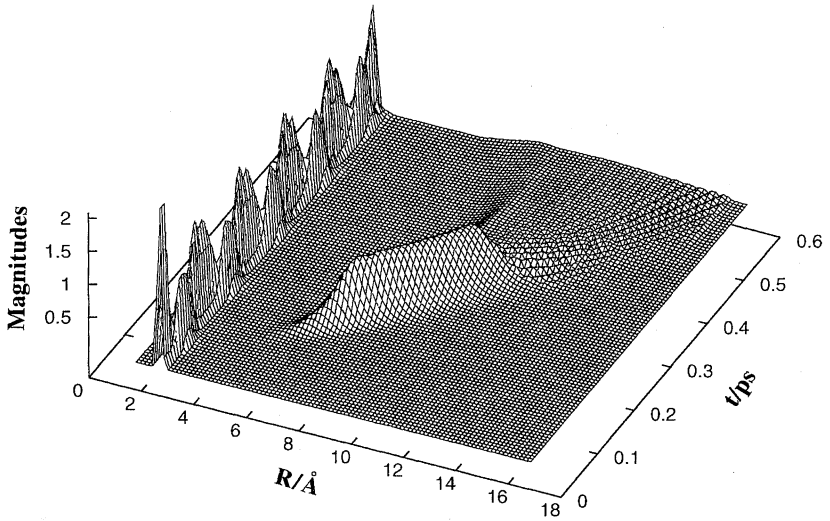

Fig. 4. Time evolution of the population in the ground state after the strong pump pulse applied. The system is expressed in terms of the diabatic representation.

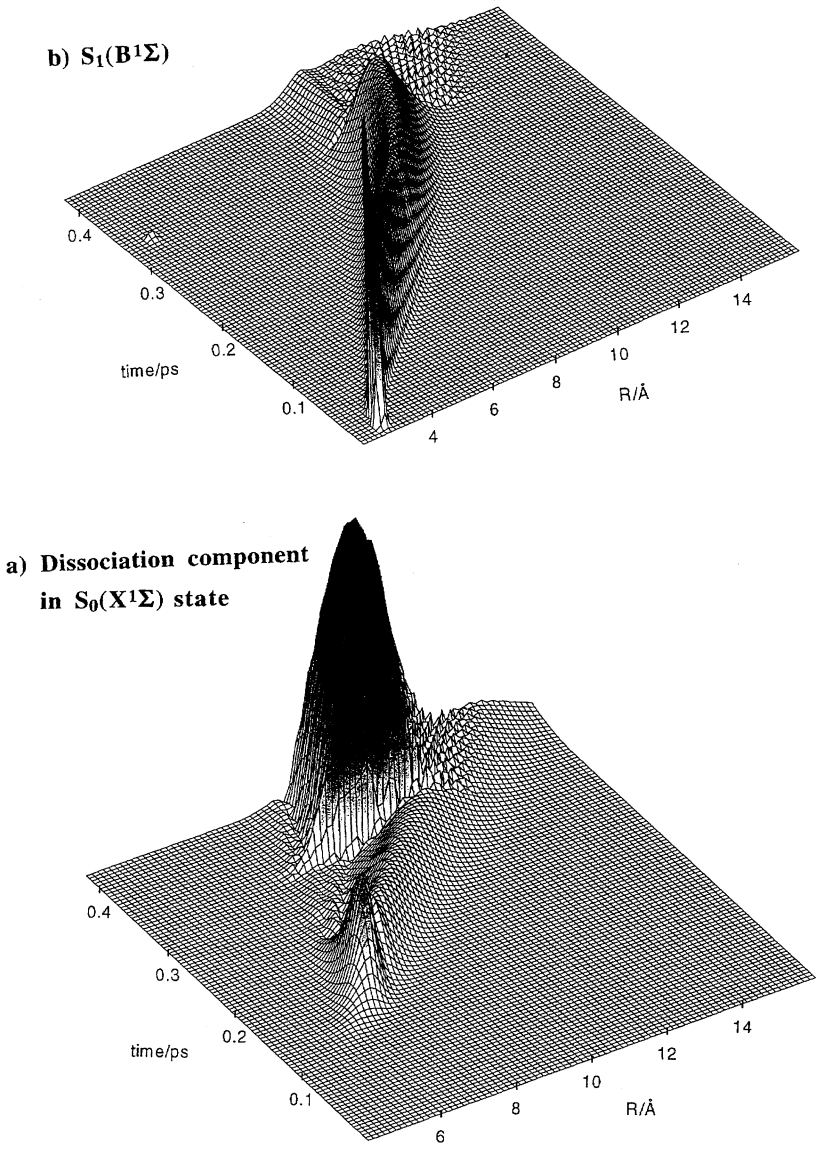

Fig. 5. a) Time evolution of the nuclear wavepacket of NaI on the ground state and b) that on the S_1 state in the strong field case. The ordinate is the absolute value of the nuclear wavepackets.

which γ is the Keldysh parameter defined in atomic units as $\gamma = \omega_L\sqrt{2I_p}/f(t)$.[55] Here, ω_L is the central frequency of the laser pulse, $f(t)$ is the pulse envelope, and I_p is the ionization potential of NaI. For the pump process, we obtain $\gamma \approx 9$ when the following parameter set is used: the resonance frequency of 4.0 eV as ω_L, 7.6 eV as I_p at the equilibrium nuclear configuration in the ground state of NaI, and the maximum field strength of 6×10^9 V m^{-1} as $f(t)$. This indicates that there is no significant contribution of tunneling ionization in the quantum control of photodissociation of NaI with laser pulses of ca. 10^9 V m^{-1}.

Weak Field Case. Figure 6 shows locally designed optimal pulses applied to NaI photodissociation in a weak field case. The maximum field strength was ca. 8×10^8 V m^{-1} for the pump pulse and 4×10^8 V m^{-1} for the dump pulse. These correspond to 29 GW cm^{-2} and 15 GW cm^{-2}, respectively. The inserted figure is the time- and frequency-resolved power spectrum of the dump pulse. We can see that the dump pulse consists of a linearly up-chirp pulse to a good approximation.

Figure 7 shows the time evolution of the population in the excited state, created by the controlled pump pulse shown in Fig. 6, and that of the photodissociation product induced by the controlled dump pulse. We can see that about 15% of the population is transferred to the final state by one stroke of the dump pulse. This relatively low yield compared with that of the strong field case described above is a common feature in pump-and-dump schemes operating under weak field conditions. It is necessary to apply to a series of dump pulses in a weak field case to obtain a high yield of population transfer.[56] We can see a small increase in the population starting after 300 fs, which is due to spontaneous predissociation, as shown in Fig. 3.

Figure 8 shows wavepacket propagations in the excited and ground states. In Fig. 8a, we can see two (fast and slow) components of the wavepacket. The fast component originates from the nonadiabatic transition and the slow one from the photodissociation induced by the controlled dump pulse. The slow velocity reflects the optical Franck–Condon principle, which involves the conservation of momentum in optical transitions. The velocity is that of the wavepacket motion of NaI in the excited state just before application of the dump pulse.

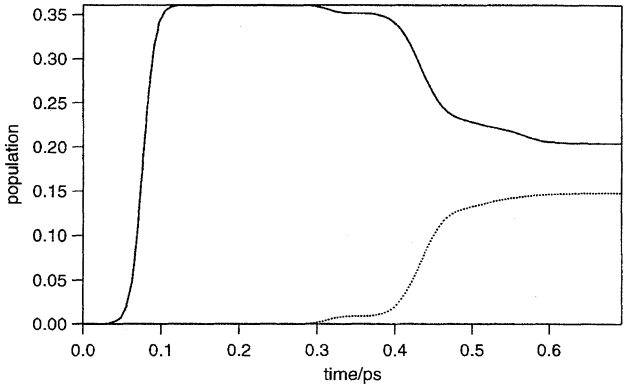

Fig. 7. The time evolution of the population in the excited state (undotted line) and that of the photodissociation product induced by the controlled dump pulse (dotted line) under the weak field condition.

In a previous paper,[52] we reported that the photodissociation of the NaI system can be controlled by applying a linearly up-chirp pulse through changing the parameters of a pump pulse without using optimization theory. In this study, we confirmed the importance of the positively chirped pulses in controlling NaI photodissociation in both weak and strong field cases based on a locally optimized control theory. The positively chirped pulses can be simply understood by a consideration of the energy difference as a function of the

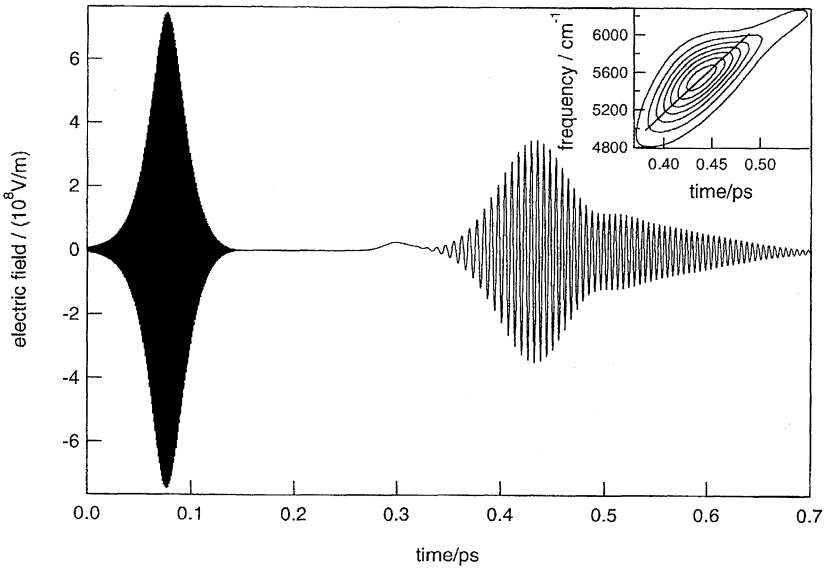

Fig. 6. Locally designed optimal pulses in a weak field case. The maximum field strength is ca. 8×10^8 V m^{-1} for the pump pulse and 4×10^8 V m^{-1} for the dump pulse. The inserted figure shows the time- and frequency-resolved power spectrum of the dump pulse. This shows that the dump pulse consists of a linearly up-chirped pulse as indicated by a line as a guide.

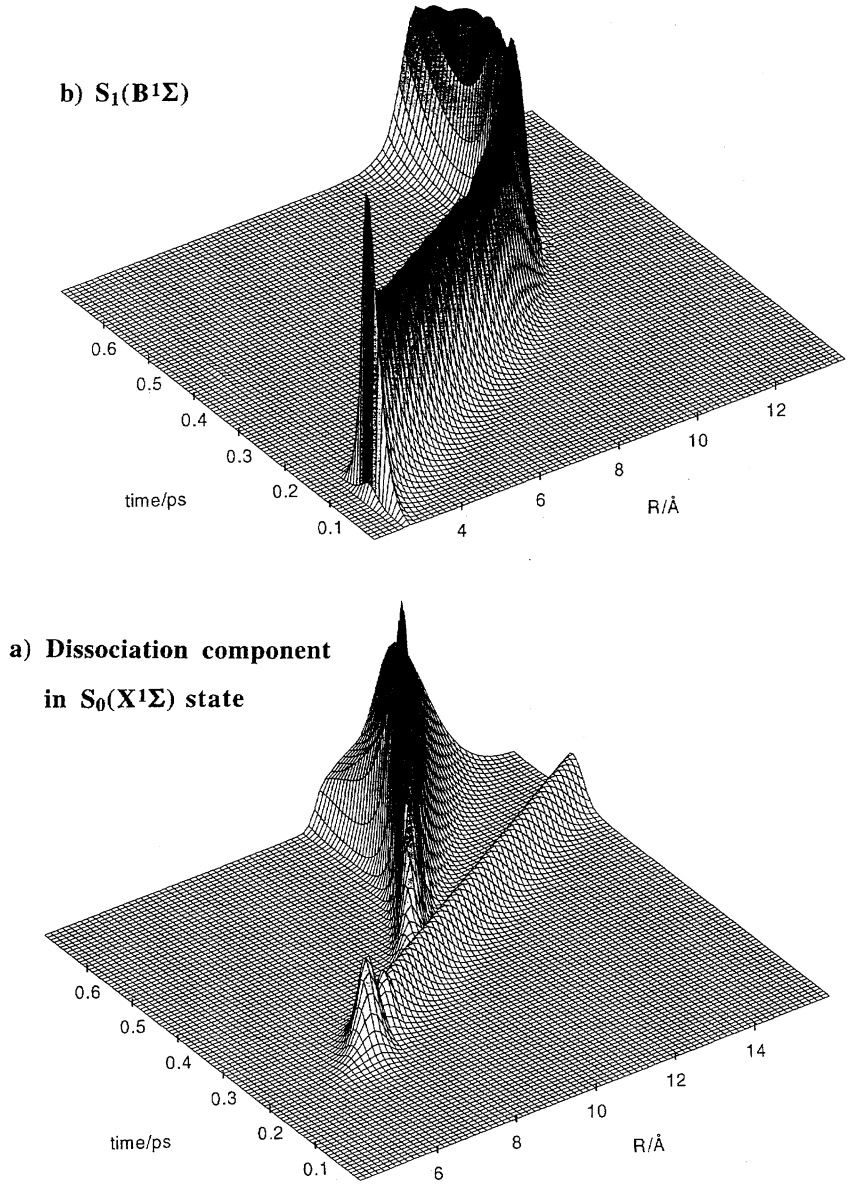

Fig. 8. a) Nuclear wavepacket propagation in the ground state, and b) nuclear wavepacket propagation in the excited state in the weak field case. Fast and slow components of the wavepacket in Fig. 8a originate from the nonadiabatic transition and from the photodissociation induced by the optimal dump pulse, respectively.

nuclear distance between the two electronic states associated with the photodissociation of NaI.

Conclusions

We have applied a locally optimized control method to the photodissociation of NaI to neutral atom fragments by a pump and dump pulse scheme. The aim of this reaction control was to obtain as many neutral fragments as possible within one cycle of the nuclear vibration. Weak and strong field cases, depending on the peak intensities of laser pulses, were considered. In both cases, the optimal dump pulses were a linear up- chirped pulse. This confirms our previous result (*Chem. Phys. Lett.*, **231**, 50 (1994)) obtained by using a non-optimal control method. The photodissociation dynamics under optimal control pulses was analyzed by nuclear wave dynamics. There exist two components in the kinetic energy of the dissociation products: one is due to the nonadiabatic transition, and the other is due to photodissociation induced by the optimal pulses. In the case of a strong laser field, a coherent excitation of vibrational eigenstates in the ionic ground-state was created as a result of stimulated emission.

One of the authors (Y. F) gratefully acknowledges the Japan Society for the Promotion of Science for their support of the Japan-Canada joint research project "Control of Reaction Dynamics by Laser." This work was partly supported by Development of High-Density Optical Pulse Generation and Advanced Material Control Techniques, and also by a Grant-in-Aid for Scientific Research (No. 09740511).

References

1 D. J. Tannor and S. A. Rice, *Adv. Chem. Phys.*, **70**, 441 (1988).

2 P. Brumer and M. Shapiro, *Annu. Rev. Phys. Chem.*, **43**, 257 (1992).

3 D. Neuhauser and H. Rabitz, *Acc. Chem. Res.*, **26**, 496 (1993).

4 B. Kohler, J. L. Krause, F. Raksi, K. R. Wilson, V.V. Yakovlev, R. M. Whitnell, and Y. J. Yan, *Acc. Chem. Res.*, **28**, 133 (1995).

5 H. Kawashima, M. M. Wefers, and K. A. Nelson, *Annu. Rev. Phys. Chem.*, **46**, 627 (1995).

6 D. Goswami, C. W. Hillegas, J. X. Tull, and W. S. Warren, "Femtosecond Reaction Dynamics," ed by D. A. Wiersma, North-Holland, Amsterdam (1994), p. 241.

7 H. Kawashima and K. A. Nelson, *J. Chem. Phys.*, **100**, 6160 (1994).

8 A. P. Heberle, J. J. Baumberg, and K. Köhler, *Phys. Rev. Lett.*, **75**, 2598 (1995).

9 M. R. Fetterman, D. Goswami, D. Keusters, W. Yang, J. -K. Rhee, and W. S. Warren, *Opt. Express*, **3**, 366 (1998).

10 W. Yang, D. Keusters, D. Goswami, and W. S. Warren, *Opt. Lett.*, **23**, 1843 (1988).

11 A. Assion, T. Baumert, M. Bergt, T. Brixner, B. Kiefer, V. Seyfried, M. Strehle, and G. Gerber, *Science*, **282**, 919 (1998).

12 I. Pastirk, E. J. Brown, Q. Zhang, and M. Dantus, *J. Chem. Phys.*, **108**, 4375 (1998).

13 R. Ubema, M. Khalil, R. M. Willams, J. M. Papanikolas, and S. R. Leone, *J. Chem. Phys.*, **108**, 9259 (1998).

14 S. Shi, A. Woody, and H. Rabitz, *J. Chem. Phys.*, **88**, 6870 (1988).

15 R. Kosloff, S. A. Rice, P. Gaspard, S. Tersigni, and D. J. Tannor, *Chem. Phys.*, **139**, 201 (1989).

16 W. Jakubetz, J. Manz, and H.-J. Schreiber, *Chem. Phys. Lett.*, **165**, 100 (1990).

17 S. Shi and H. Rabitz, *J. Chem. Phys.*, **92**, 364 (1990).

18 P. Gross, D. Neuhauser, and H. Rabitz, *J. Chem. Phys.*, **96**, 2834 (1992).

19 P. Gross, D. Neuhauser, and H. Rabitz, *J. Chem. Phys.*, **98**, 4557 (1993).

20 J. L. Krause, R. M. Whitnell, K. R. Wilson, Y. Yan, and S. Mukamel, *J. Chem. Phys.*, **99**, 6562 (1993).

21 Y. Yan, R. E. Gillian, R. M. Whitnell, K. R. Wilson, and S. Mukamel, *J. Phys. Chem.*, **97**, 2320 (1993).

22 L. Shen, S. Shi, and H. Rabitz, *J. Phys. Chem.*, **97**, 8874 (1993).

23 L. Shen, S. Shi, and H. Rabitz, *J. Phys. Chem.*, **97**, 12114 (1993).

24 L. Shen and H. Rabitz, *J. Chem. Phys.*, **100**, 4811 (1994).

25 M. Sugawara and Y. Fujimura, *J. Chem. Phys.*, **100**, 5646 (1994).

26 M. Sugawara and Y. Fujimura, *J. Chem. Phys.*, **101**, 6586 (1994).

27 M. Sugawara and Y. Fujimura, *Chem. Phys.*, **196**, 113 (1995).

28 V. Dubov and H. Rabitz, *Chem. Phys. Lett.*, **235**, 309 (1995).

29 J. Botina, H. Rabitz, and N. Rahman, *J. Chem. Phys.*, **102**, 226 (1995).

30 V. Dubov and H. Rabitz, *J. Chem. Phys.*, **103**, 8412 (1995).

31 J. Botina, H. Rabitz, and N. Rahman, *J. Chem. Phys.*, **104**, 4031 (1996).

32 X. Jiang, M. Shapiro, and P. Brumer, *J. Chem. Phys.*, **104**, 607 (1996).

33 Y. Watanabe, H. Umeda, Y. Ohtsuki, H. Kono, and Y. Fujimura, *Chem. Phys.*, **217**, 317 (1997).

34 Y. Ohtsuki, H. Kono, and Y. Fujimura, *J. Chem. Phys.*, **109**, 2032 (1998).

35 Y. Teranishi and H. Nakamura, *Phys. Rev. Lett.*, **81**, 9318 (1998).

36 J. C. Polanyi and A. H. Zewail, *Acc. Chem. Res.*, **28**, 119 (1995).

37 M. J. Rosker, T. S. Rose, and A. H. Zewail, *Chem. Phys. Lett.*, **146**, 175 (1988).

38 V. Engel, H. Metiu, R. Almeida, R. A. Marcus, and A. H. Zewail, *Chem. Phys. Lett.*, **152**, 1 (1988).

39 T. S. Rose, M. J. Rosker, and A. H. Zewail, *J. Chem. Phys.*, **91**, 7415 (1989).

40 V. Engel and H. Methiu, *J. Chem. Phys.*, **90**, 6116 (1989).

41 P. Cong, A. Mokhtari, and A. H. Zewail, *Chem. Phys. Lett.*, **172**, 109 (1990).

42 H. Kono and Y. Fujimura, *Chem. Phys. Lett.*, **184**, 497 (1991).

43 J. L. Herek, A. Materny, and A. H. Zewail, *Chem. Phys. Lett.*, **228**, 15 (1994).

44 T. Taneichi, T. Kobayashi, Y. Ohtsuki, and Y. Fujimura, *Chem. Phys. Lett.*, **231**, 50 (1994).

45 C. J. Bardeen, J. Che, K. R. Wilson, V. V. Yakovlev, P. Cong, B. Kohler, J. L. Krause, and Messina, *J. Phys. Chem. A*, **101**, 3815 (1997).

46 H. Tang and S. A. Rice, *J. Phys. Chem. A*, **101**, 9587 (1997).

47 K. Mishima and K. Yamashita, *J. Mol. Struct.*, (*THEOCHEM*), **461—462**, 483 (1999).

48 K. Hoki, Y. Ohtsuki, H. Kono, and Y. Fujimura, *J. Phys. Chem. A*, **103**, 6301 (1999).

49 M. W.Schmidt, K. K. Baldridge, J. A. Boatz, S. T. Elbert, M. S. Gordon, J. H. Jensen, S. Koseki, N. Matsunaga, K. A. Nguyen, S. Su, T. L. Windus, M. Dupuis, and J. A. Montgomery, Jr., *J. Comput. Chem.*, **14**, 1347 (1993).

50 H.-J. Werner and P. J. Knowles, "MOLPRO program code," 1992.

51 S. Chelkowski, A. D. Bandrauk, and P. B. Corkum, *Phys. Rev. Lett.*, **65**, 2355 (1990).

52 J. E. Combariza, S. Görtler, B. Jusut, and J. Manz, *Chem. Phys. Lett.*, **195**, 393 (1992).

53 K. Mishima and K. Yamashita, *J. Chem. Phys.*, **109**, 1801 (1998).

54 M. Sugawara and Y. Fujimura, *Chem. Phys.*, **175**, 323 (1993).

55 S. August, D. D. Meyerhofer, D. Strickland, and S. L. Chin, *J. Opt. Soc. Am.*, **B8**, 858 (1991).

56 Y. Ohtsuki, Y. Yahata, H. Kono, and Y. Fujimura, *Chem. Phys. Lett.*, **287**, 627 (1998).